POLITECNICO
MILANO 1863

RE.PUBLIC@POLIMI
Research Publications at Politecnico di Milano

This is the published version of:

I. Bayati, L. Bernini, A. Zanotti, M. Belloli, A. Zasso
Experimental Investigation of the Unsteady Aerodynamics of FOWT Through PIV and Hot-Wire Wake Measurements
Journal of Physics: Conference Series, Vol. 1037, 2018, p. 1-11
doi:10.1088/1742-6596/1037/5/052024

The final publication is available at http://dx.doi.org/10.1088/1742-6596/1037/5/052024

When citing this work, cite the original published paper.

Permanent link to this version
http://hdl.handle.net/11311/1057000

Journal of Physics: Conference Series

PAPER • **OPEN ACCESS**

Experimental investigation of the unsteady aerodynamics of FOWT through PIV and hot-wire wake measurements

To cite this article: I. Bayati *et al* 2018 *J. Phys.: Conf. Ser.* **1037** 052024

View the article online for updates and enhancements.

Related content

- Nonlinear wave effects on dynamic responses of a semisubmersible floating offshore wind turbine in the intermediate water
  Jia Pan and Takeshi Ishihara
- Alternative linearisation methodology for aero-elastic Floating Offshore Wind Turbine non-linear models
  Joannes Olondriz, Josu Jugo, Iker Elorza et al.
- Numerical analysis of unsteady aerodynamics of floating offshore wind turbines
  M. Cormier, M. Caboni, T. Lutz et al.

This content was downloaded from IP address 131.175.12.9 on 22/06/2018 at 10:39

IOP Conf. Series: Journal of Physics: Conf. Series **1037** (2018) 052024 doi:10.1088/1742-6596/1037/5/052024

Experimental investigation of the unsteady aerodynamics of FOWT through PIV and hot-wire wake measurements

I.Bayati[1*], L.Bernini[1], A.Zanotti[2], M.Belloli[1] & A.Zasso[1]

1:Politecnico di Milano, Department of Mechanical Engineering, Milano, Italy
2:Politecnico di Milano, Department of Aerospace Engineering, Milano, Italy

E-mail: ilmasandrea.bayati@polimi.it

Abstract. This work presents a selected set of results from an extensive experimental campaign aimed at characterizing the wake aerodynamics of a floating offshore wind turbines (FOWT) in dynamic conditions. The campaign was carried out in the Politecnico di Milano 14m x 4m atmospheric boundary layer test section, under UNAFLOW project (UNsteady Aerodynamics of FLoating Wind turbines). Wake measurements were carried out either through hot-wire anemometers with a traversing system as well as through Particle Image Velocimetry (PIV) technique. A 1/75 scale model of the DTU 10 MW reference wind turbine was adopted, which was mounted on a hydraulically actuated mechanism imposing sinusoidal surge motion at different frequencies and amplitudes, and for different tip speed ratios λ. Selected results are reported with the aim of giving a first interpretation of the novel set of measurements, also completing previous measurements conducted by the authors, to put the basis of a more comprehensive understanding of unsteady aerodynamics of FOWT for control and wind farm purposes.

1. Introduction

Wind turbines' design is recently moving to large multi-megawatt rotors. This requires unsteady aerodynamics to be taken into account due to very long and flexible blades, not to mention the floating offshore applications which makes also the platform's motion contribute to the varying effective wind velocity seen by the rotor. In this scenario, the fully understanding of the complexity of unsteady aerodynamics and of its fallout in the aero- and servo-elastic response of such machines, are still far from being accomplished.

Recent relevant projects have been investigating the problem of relying on advanced numerical tools to be predictive of the aerodynamics of up-scaled rotors up to 10-20 MW, such as AVATAR [1]. Most recently, the unsteady aerodynamics has emerged as a fundamental issue to be accounted for in floating offshore wind from wind tunnel measurements ([3], [4]), for its contribution in the global dynamics and control of such machines; simplified formulations have been proposed [2], with a reduced-order modelling approach for inclusion in the early design phases or eve in model predictive control.

The present UNAFLOW project (UNsteady Aerodynamics of FLoiating Wind turbines) [6], [7] was aimed at improving this experimental and numerical database through advanced measurements at Politecnico di Milano Wind Tunnel through Particle Image Velocimetry (PIV)

Content from this work may be used under the terms of the Creative Commons Attribution 3.0 licence. Any further distribution of this work must maintain attribution to the author(s) and the title of the work, journal citation and DOI.
Published under licence by IOP Publishing Ltd

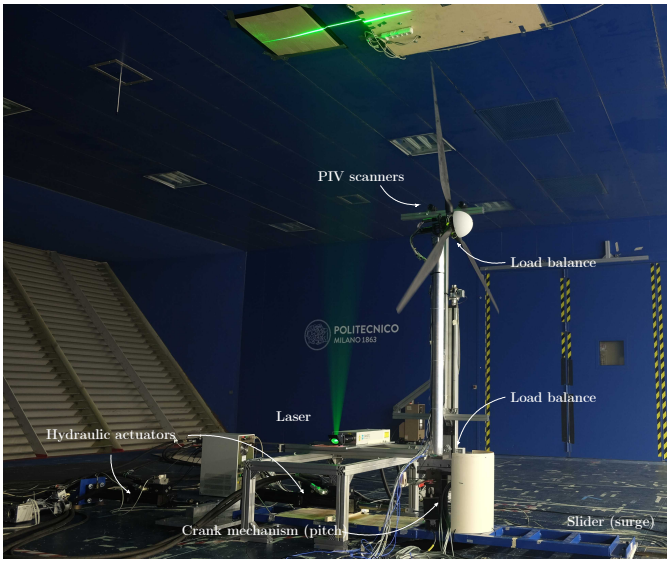

Figure 1. Test rig.

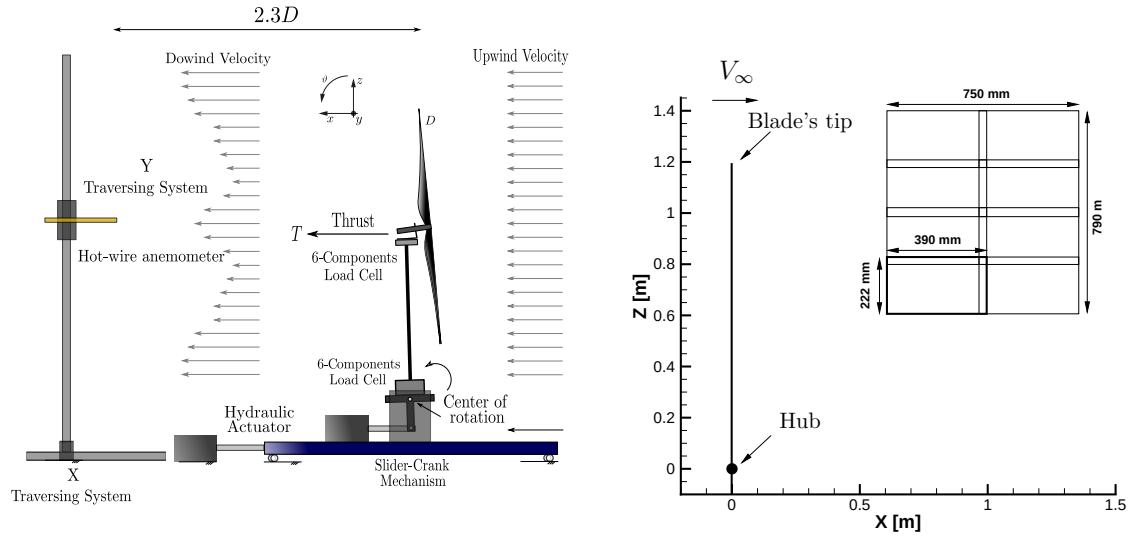

Figure 2. Sketch of the hot-wire anemometric setup (left) and PIV test rig (right - layout and positioning of the PIV measurement planes, the dimensions of the measurement windows are shown for the lower-left window).

and high-fidelity modelling (CFD) to get deeper insight into the unsteady aerodynamics for multi-megawatt floating wind turbines.

2. Experimental set-up

2.1. Wind turbine model

The wind turbine adopted during the tests is a 1/75 aero-elastic scale model of the reference DTU 10MW, risulting in a 2.38 m of diameter D, where SD7032 low-reynolds profiles have been adopted to replace the full scale FFA series airfoils. More details about the aero-structural

design can be found in [8], as well for the mechatronic design of the model [9]. Measurements of the aerodynamic forces on the model were possible by means of the 6-components balances at the tower's top and base, as reported in Fig.1 and 2.

2.2. Hot-wire anemometry set-up

The wake generated by the wind turbine was measured by an automatic traversing mechanism employing tri-axial sensor probe hot-wire anemometers. The sensors could measure the three wind velocity components *(u,v,w)*. In Fig.1 and 2 a sketch of the traversing system with the mounted hot-wire probe is reported. Measurements were conducted with the traversing system either spanning along cross-wind direction (Y) and along-wind (X), respectively moving the probe at hub's height from -1.6 m to +1.6 m at a given 2.3D fixed downwind distance, as well as along wind, ranging from 0.9D to 2.3D, at a given a 0.75R radial fixed position, where R is the wind turbine's radius. The cross-wind measurements have been performed with a spatial discretization of 100 mm (33 points), whereas the along-wind measurements by 330 mm (10 points).

2.3. PIV set up

The near-wake of the wind turbine scaled model was investigated by means of 2D PIV surveys carried out for test conditions with and without surge motion. The employed PIV instrumentation was composed by a Nd:YAG double pulsed laser with 200 mJ output energy and a wavelength of 532 nm and two adjacent cameras with a 12-bit, 1952 $\times$ 1112 pixel array equipped with a 50 mm lens. A view of the PIV set up in the wind tunnel test section is shown in Fig. 1 and Fig.2.

The laser was installed on a support parallel to the floor so as the light sheet was aligned with the longitudinal vertical plane passing through wind turbine hub centerline ($X-Z$ plane). The origin of the reference system is positioned at rotor hub center. The cameras line of sight was perpendicular to the laser sheet. The total area of investigation was 0.75 m wide and 0.79 m high. In order to achieve better resolution of the image pairs, the measurement area was composed by eight windows (0.39 m wide and 0.22 m high) arranged as four rows and two columns with a small overlapping band between them. Thus, the cameras are mounted on a vertical axis traversing system to cover the entire area of measurement. The arrangement and positioning of the measurement windows are depicted in the sketch shown in Fig. 2 and Fig.1. The outer edge of the measurement area was located at half radius past the rotor disk with the wind turbine in steady position.

The test chamber was fulfilled with the seeding using two particle generators with Laskin atomizer nozzles (PIVpart30 by PIVTEC) located in the return duct of the wind tunnel to avoid disturbance to the measurements. The particles consisted of small DEHS oil droplets with a diameter in the range of 1-2 μm. The image pair analysis was carried out using PIVview 3C software [11], developed by PIVTEC in close cooperation with the PIV-Groups of the German Aerospace Center (DLR) in Gottingen and Koln. The image pairs were post-processed using the multigrid interrogation algorithm [12] leading to a resolution of a measurement point every 7 mm. The accuracy of the present PIV measurements can be estimated considering a maximum displacement error of 0.1 pixels [13]. Thus, taking into account the employed pulse-separation time and the optical magnification [14], the maximum in-plane velocity components error of the present measurements is about 0.07 m/s. The number of image pairs considered in the present PIV campaign for each measurement window was a compromise to limit the acquisition time due to the large number of test conditions and the amplitude of the investigation area. Consequently, the statistical error related to the limited number of image pairs used for the phase-averaged process should be higher than the evaluated bias error (0.07 m/s).

The synchronization of the two laser pulses with the image pair exposure was controlled by a 6-channels Quantum Composer QC9618 pulse generator while the digital images were captured using a GigaEthernet EBus connection. A different strategy for the image capturing was used for the test with the wind turbine in steady condition with respect to the ones with surge motion. For steady tests phase-locked measurements were carried out over the entire rotation cycle of the rotor by synchronizing the laser pulses with a prescribed azimuthal position (ψ) of a master blade (1/rev signal). In particular, PIV measurements were carried out from $\psi = 0°$ to $\psi = 120°$ with a 15° step and from $\psi = 120°$ to $\psi = 360°$ with a 30° step. For these tests one hundred image pairs were acquired for each measurement window to obtain the phase-averaged flow field at each considered azimuthal position of the master blade. This strategy enabled to investigate the spatial evolution of the blade tip vortices with respect to the blade rotation [15].

For the tests surge motion phase-locked measurements were carried out by synchronizing the laser pulses with several prescribed positions of the wind turbine along the entire motion cycle in surge. The horizontal displacement of the wind turbine along surge motion is indicated with h. In particular, $h = 0$ mm corresponds to the wind turbine at maximum advancing velocity, thus with phase $\phi = 0°$ along the sinusoidal surge motion cycle. For these tests image pairs were acquired over fifty cycles of the surge motion for each measurement window to obtain the phase-averaged flow field at each considered position h of the wind turbine along the surge cycle. The aim of this strategy was to evaluate the effect of the surge motion on the average near wake of the wind turbine. Moreover, the data base collected for these tests enabled to isolate the flow field measured at several positions along a single surge motion cycle but at the same prescribed azimuthal position of the master blade. This post-processing technique enabled to evaluate the effect of the surge motion on the spatial evolution of the blade tip vortex.

3. Results and discussion

The PIV surveys were carried out with a rotational speed Ω of the wind turbine rotor of 241 rpm and a wind tunnel free-stream velocity U_∞ of 4 m/s. In PIV results representations the vertical line depicted in the following figures indicates the position of the rotor disk. Moreover, the data contained in two small rectangular regions at the lower-left and lower-right corner of the investigation area were blanked as they were considered as outliers due to the poor level of power at the edges of the laser sheet.

Figure 3 shows the averaged flow fields measured with no motion of the wind turbine phase-locked at different azimuthal positions of the master blade. This test condition is useful as reference condition to appreciate the effect of FOWT motion on the near wake flow field. In particular, the contours of the velocity component along X axis (u) and the higher and lower velocity regions clearly indicate the position of the tip vortices as released by the three rotor blades with respect to the azimuthal phase of the master blade. Moreover, the entire measurement window illustrates the topology of the near wake past the wind turbine, both the velocity deficit area behind the rotor and the speed up in the outer region are captured by the PIV images. In order to highlight the effect of the surge motion on the spatial evolution of the blade tip vortices, Fig. 4 shows the comparison between PIV results measured in steady condition (see Fig. 4a) and with imposed surge motion (with frequency $f = 0.5$ Hz and amplitude $A = 65$ mm) at the same prescribed azimuthal position of the master blade $\psi = 0°$ (see Fig. 4b-d). In particular, the contours of the vorticity magnitude ω calculated using the in-plane velocity components (u,v) are illustrated to better highlight the displacement of the tip vortices core along the surge cycle. The PIV images are arranged in a single column to improve the readability of the vortices displacement. As previously mentioned, the PIV results shown in Fig. 4b-d are not averaged as they are evaluated along a single surge cycle at different h positions of the wind turbine.

The comparison of Fig. 4a and Fig. 4c shows that the tip vortices core position for surge

motion at $\phi = 0°$ is close to the one evaluated with the wind turbine in steady condition at the same blade azimuthal phase $\psi = 0°$. On the other hand, Figs. 4b-d shows that the tip vortices core moves according to the imposed surge motion. In particular, the amplitude of the tip vortices core displacement is close to the surge motion amplitude. Moreover, Fig. 4e and Fig. 4h show that the outer locations of the tip vortices core are not reached in correspondence of zero velocity of the wind turbine along the surge motion cycle (see Fig. 4d at $\phi = 90°$ and Fig. 4g at $\phi = 270°$). This delay is related to the fact that the vortices travel into the measurement area, located about one rotor radius past the disk, with a velocity close to the free-stream.

With regard to Fig.5, the comparison is reported handling the unsteady measurements by averaging over platform motion's cycles independently from the blade's azimuthal position. A set of platform's position's h (corresponding to sine wave' phases ϕ) are reported. It is evident how hard is to draw any conclusion about the dynamic wake's structures since the information on the tip's vorticity is being smeared by this data processing. This suggests that the approach reported in Fig. 4 is preferred, although requires to have the rotor frequency multiple of the frequency of motion, so as to have at least a subset of motion's phases with the same azimuthal position of the previous cycle.

In Fig.6-Fig.7 results from hot-wire measurements are reported. The time histories were gathered through 60 seconds of acquisition for having a discrete number of periods for each different tested frequency of motion, and sampled by f_{samp} of 2k Hz. The unsteady and steady spectra are compared to each other under the form of spectrograms. Fig.6 is for a given cross-wind (2.3D), whereas Fig.7 is for a fixed y position (0.75R) and different downwind positions.

In Fig.6, $y = 0$ refers to the hub position; the most evident aspect, it's that both steady and unsteady results show the highest energy content, over a wide frequency range, in a region close to the blades' tips. It is clearly visible how the frequency component due to the motion is present in the wake measurements, at 2.3D downwind distance, especially in the along-wind component u.

A defined harmonic content at rotational frequency is present probably due to some aerodynamic imbalance of the rotor blades (possibly a small pitch angle difference). The plot is limited at 5 Hz since no trace of the 3P (three times the rotational frequency) is visible . For the presented conditions the rotor is in the rated region resulting in low wake speed which make difficult the measurement of the three vortex filaments at the sampled distance. For different conditions, not presented here, with lighter loaded rotor and higher wake speed the 3P was measured, also the PIV images, made closer to the rotor plane, showed clearly three different vortex cores, see Fig.4.

In Fig.7 the same consideration of Fig.6 hold; however, it can also be noticed that the more the downwind distance, the more the energy content is smeared out over a greater frequency range. On the contrary the vertical and cross-wind velocity components in the unsteady conditions, seem to be increasing at the frequency of platform motion.

4. Conclusions

This paper presented reported a first analysis of advanced wind tunnel measurements on floating offshore wind turbines, aimed at assessing the physics behind the complex unsteady aerodynamics. PIV and hot-wire anemometry was set to investigate steady and unsteady wake dynamics for different amplitudes and frequency of motions. From this first analysis what is emerging can be summarized in the following. Regarding the hot-wire measurements, the frequency of motion is clearly visible in the downwind wake and it is added onto the steady response in a quite clean manner. Along wind measurements showed that the energy content is smeared over a wider range of frequencies expect for the cross-wind component at the frequency of motion.

With regard to PIV measurements, tracking the vorticity (averaging over cycles for given

azimuthal positions of the blades) gives a good indication on the of the dynamics of the wake under in unsteady conditions, whereas averaging for a given platform position independently the blade azimuthal angle seems not to be recommended since the wake structure due the motion is smoothed out. Nevertheless, regarding the former approach for PIV data elaboration, this is possible only for frequency of rotor's angular rotation multiple of the platform frequency of motion, as the case analysed in this paper, so that reproducing in wind tunnel experiments this condition seems to be the best way to observe wake structures in the unsteady wakes of floating offshore wind turbines.

Measurements reported suggest also that PIV observation windows can be set better around the tip vortices since no relevant information, even in the dynamic wake, is visible closer to the wind turbine's shaft.

Aknowledgments

This research has been funded by EU-EERA (European Energy Research Alliance)/IRPWIND Joint Experiment 2017.

References

[1] J. G. Schepers , O. Ceyhan , F. J. Savenije, M. Stettner, H. J. Kooijman, T. Chaviarapolous, G. Sieros, C. Ferreira, N. Srensen, M. Wchter, B. Stoevesandt, T. Lutz, A. Gonzalez, G. Barakos, A. Voutsinas, A. Croce, J. Madsen, AVATAR: AdVanced Aerodynamic Tools for lArge Rotors, 33rd Wind Energy Symposium - AIAA SciTech 2015, 2015, ISBN: 9781624103445, p. 1-20, AIAA 2015-0497 , DOI: 10.2514/6.2015-0497, 2015.

[2] I. Bayati, M. Belloli, L. Bernini, A.Zasso "A formulation for the unsteady aerodynamics of floating wind turbines, with focus on the global system dynamics" *Proceedings of the International Conference on Offshore Mechanics and Arctic Engineering - OMAE 2017.*

[3] I. Bayati, M. Belloli, L. Bernini, A. Zasso, Wind tunnel validation of AeroDyn within LIFES50+ project: imposed Surge and Pitch tests, Journal of Physics Conference Series 753(9), October 2016. DOI: 10.1088/1742-6596/753/9/092001

[4] I. Bayati, M. Belloli, L. Bernini, A. Zasso, "Wind tunnel wake measurements of floating offshore wind turbines" (2017) Energy Procedia 137:214-222, pp. 214-222.

[5] Politecnico di Milano Wind Tunnel: `www.windtunnel.polimi.it`

[6] I.Bayati, M. Belloli, L.Bernini, D.Boldrin, K.Boorsma, M.Caboni, M.Cormier, R.Mikkelsen, M.Serdeczny, T. Lutz, A.Zasso, "UNAFLOW project: UNsteady Aerodynamics of FLOating Wind turbines", The Science of Making Torque From Wind 2018, Journal of Physiscs - IOP Conference Series.

[7] UNAFLOW project/repository: `www.unaflow.mecc.poliimi.it`

[8] Bayati I, Belloli M, Bernini L and Zasso A 2017 Aerodynamic design methodology for wind tunnel tests of wind turbine rotors *Journal of Wind Engineering and Industrial Aerodynamics*, **167** pp 217-227.

[9] I. Bayati; M. Belloli; L. Bernini; H. Giberti; Zasso, A.: 'Scale model technology for floating offshore wind turbines', IET Renewable Power Generation, 2017, DOI: 10.1049/iet-rpg.2016.0956 IET Digital Library

[10] Campanardi G, Grassi D, Zanotti A, Nanos EM, Campagnolo F, Croce A and Bottasso CL 2017 Stereo particle image velocimetry set up for measurements in the wake of scaled wind turbines *Journal of Physics: Conference Series*, **882** 012003.

[11] PIVview 2C/3C, User Manual, PIVTEC, www.pivtec.com

[12] Raffel M, Willert C, Wereley S and Kompenhans J 2007 *Particle Image Velocimetry - A Practical Guide* (Berlin:Springer Verlag)

[13] Zanotti A, Ermacora M, Campanardi G and Gibertini G 2014 Stereo Particle Image Velocimetry Measurements of Perpendicular Blade-Vortex Interaction over an Oscillating Airfoil *Experiments in Fluids* **55**(9) pp 1-13

[14] De Gregorio F, Pengel K and Kindler K 2012 A comprehensive PIV measurement campaign on a fully equipped helicopter model *Experiments in Fluids* **53** pp 37-49

[15] Droandi G, Zanotti A and Gibertini G 2015 Aerodynamic Interaction Between Rotor and Tilting Wing in Hovering Flight Condition *Journal of the American helicopter Society* **60**(4) pp 1-20

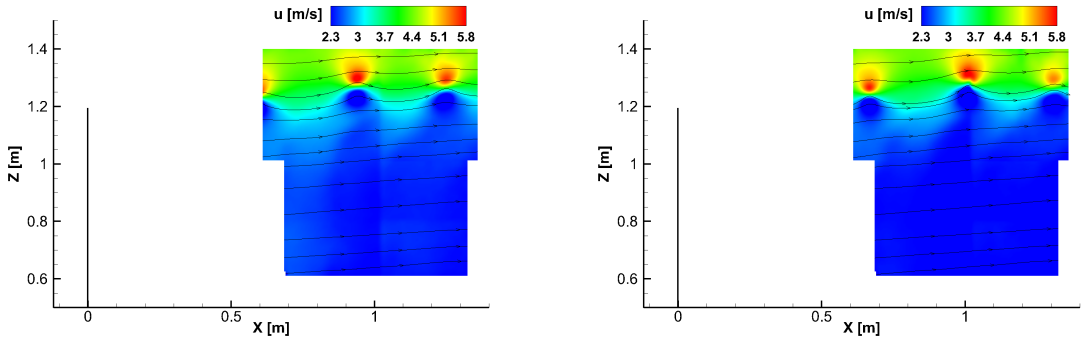

(a) $\psi = 0°$ (b) $\psi = 30°$

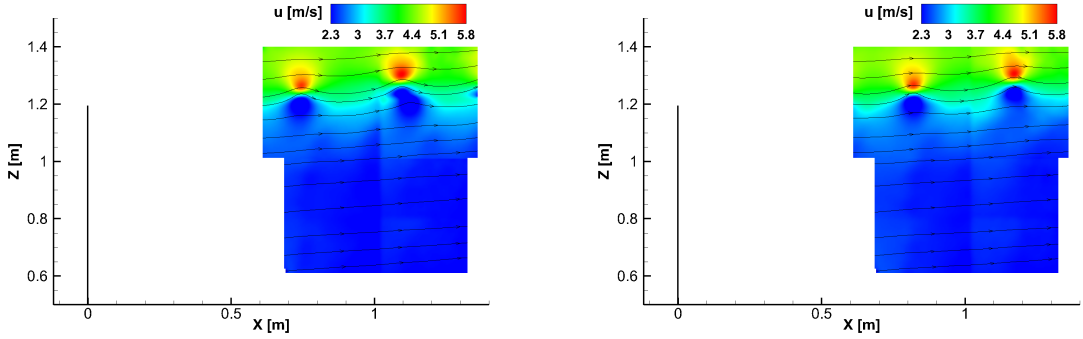

(c) $\psi = 60°$ (d) $\psi = 90°$

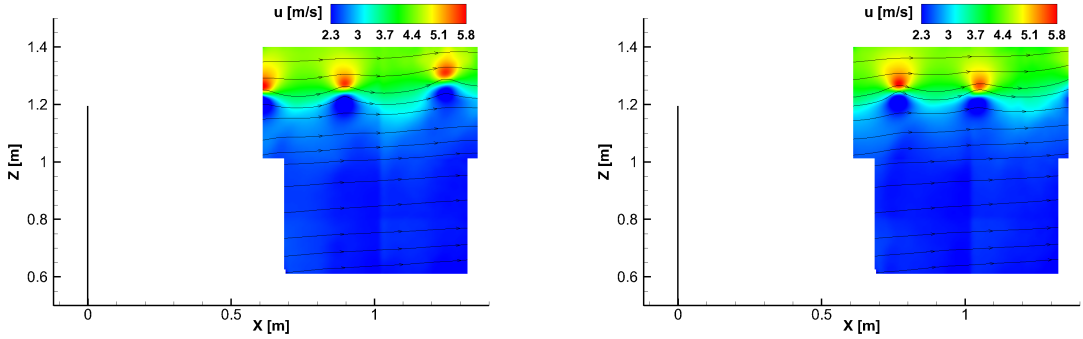

(e) $\psi = 120°$ (f) $\psi = 180°$

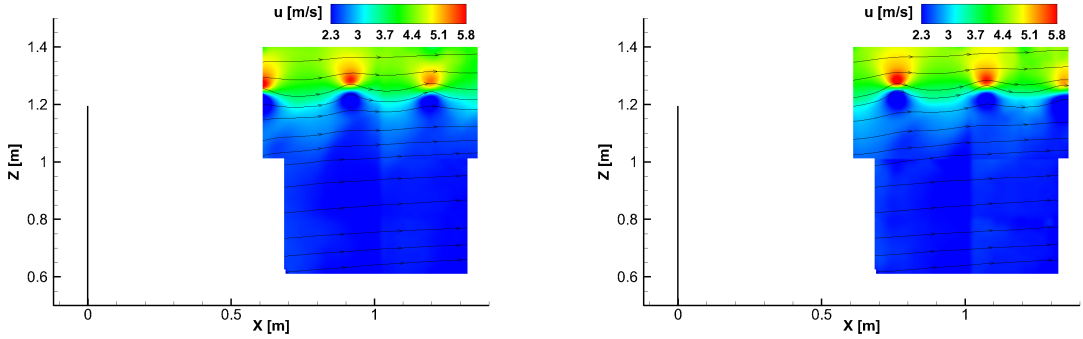

(g) $\psi = 240°$ (h) $\psi = 300°$

Figure 3. PIV results for wind turbine model in steady condition ($\Omega = 241$ rpm, $U_\infty = 4$ m/s): u velocity component contours

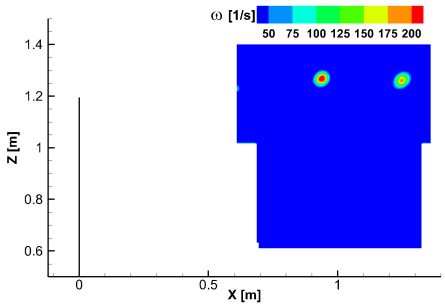

(a) $\psi = 0°$, $\phi = 0°$, $h = 0$ mm, steady

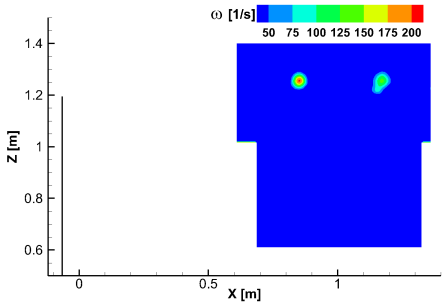

(b) $\psi = 0°$, $\phi = 90°$, $h = -65$ mm, surge

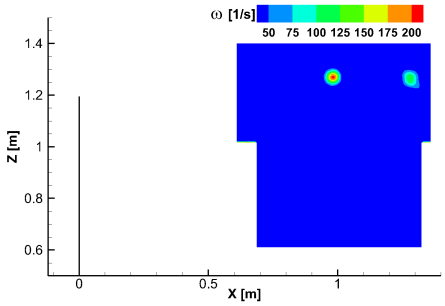

(c) $\psi = 0°$, $\phi = 0°$, $h = 0$ mm, surge

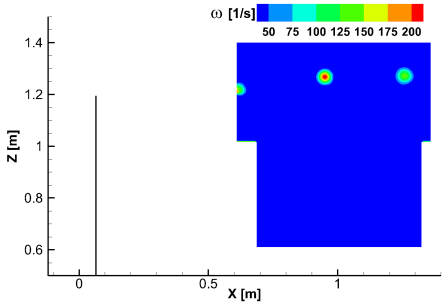

(d) $\psi = 0°$, $\phi = 270°$, $h = 65$ mm, surge

Figure 4. Comparison between PIV results for wind turbine model in steady condition (averaged on 100 rotor cycles) and with imposed surge motion (single sinusoidal cycle with $f = 0.5$ Hz, $A = 65$ mm) at $\psi = 0°$ ($\Omega = 241$ rpm, $U_\infty = 4$ m/s): ω vorticity magnitude contours

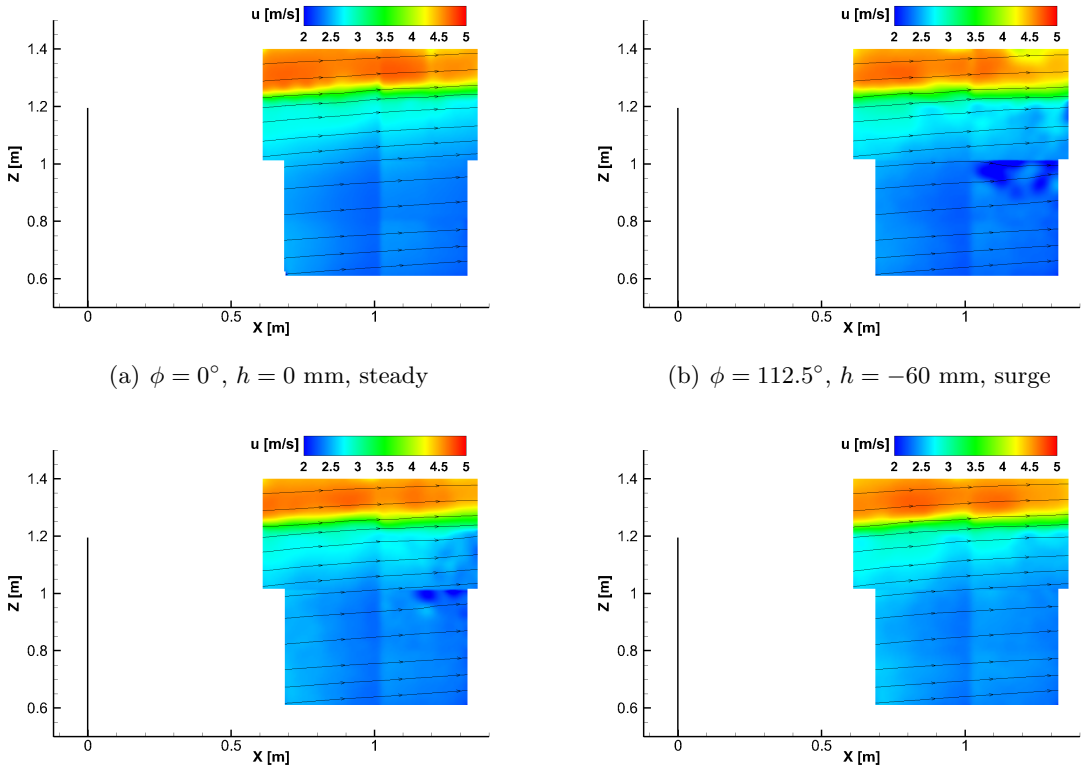

(a) $\phi = 0°$, $h = 0$ mm, steady

(b) $\phi = 112.5°$, $h = -60$ mm, surge

(c) $\phi = 180°$, $h = 0$ mm, surge

(d) $\phi = 292.5°$, $h = 60$ mm, surge

Figure 5. Comparison between PIV averaged results for wind turbine model in steady condition (ensemble averaged on all the azimuthal positions of the blade acquired) and with imposed surge motion (phase-averaged over 50 surge sinusoidal cycles with $f = 0.5$ Hz, $A = 65$ mm) ($\Omega = 241$ rpm, $U_\infty = 4$ m/s): ω vorticity magnitude contours

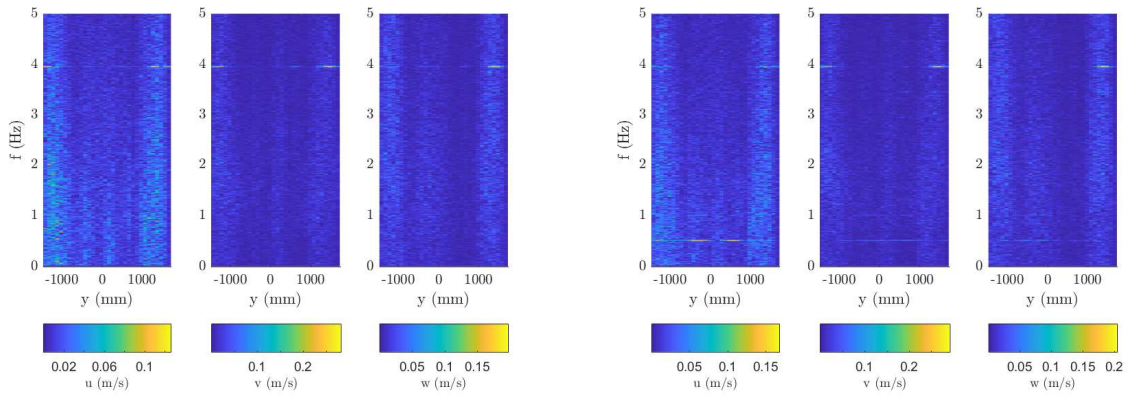

Figure 6. Spectrograms of the wind velocity components about cross-wind measurements, for the steady (left) and unsteady condition (right) - $f = 0.5$ Hz, $A = 65$ mm.

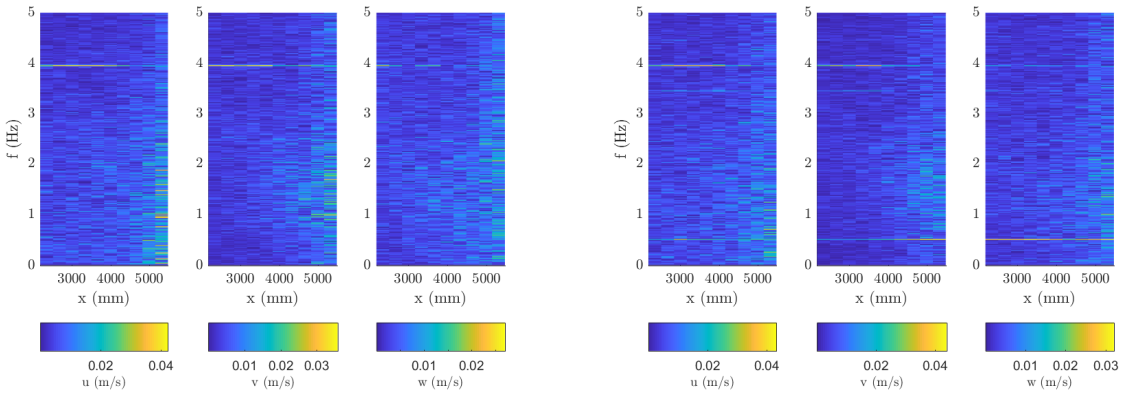

Figure 7. Spectrograms of the wind velocity components about along wind measurements, for the steady (left) and unsteady condition (right) - $f = 0.5$ Hz, $A = 65$ mm.